

Controlling Material Properties in new Phase Change Alloys beyond the pseudobinary line

Wojciech Welnic^{1,2,3}, Daniel Lüsebrink¹, Daniel Wamwangi¹, Michael Gilleßen⁴,
Richard Dronskowski⁴ and Matthias Wuttig¹

¹*I. Physikalisches Institut IA, RWTH Aachen, 52056 Aachen, Germany*

²*Laboratoire des Solides Irradiés, École Polytechnique, Palaiseau, France*

³*European Theoretical Spectroscopy Facility (ETSF)*

⁴*Institut für Anorganische Chemie, RWTH Aachen, 52056 Aachen, Germany*

1 Introduction

The electronic properties of semiconductors can be manipulated over a wide range by proper doping and an expert control of defects. Intrinsic defects such as vacancies or interstitials found in semiconductors like Si, Ge or GaAs have rather high formation energies, e.g., in Si the formation energy for a vacancy has been calculated to 3.3 eV[1]. Surprisingly enough, however, there is a whole class of chemically more complex semiconductors which possess huge vacancy concentrations even at conditions close to thermodynamic equilibrium. This implies that these vacancies should be an intrinsic feature of the alloys. The materials discussed here are Te based phase change alloys which are presently employed for rewritable data storage[2] and are a promising candidate for non-volatile electronic memories[3]-[5].

These materials are characterized by a remarkable property combination. They show a pronounced contrast of optical and electronic properties between the amorphous and crystalline state, indicative for a pronounced structural difference between these two states[6],[7]. At the same time the crystallization of the amorphous state proceeds very rapidly. A prototype phase change material is $\text{Ge}_2\text{Sb}_2\text{Te}_5$, which forms a metastable crystalline state with a rocksalt-like structure. Understanding this metastable structure is crucial for an understanding of phase change materials, since the fast phase transformation proceeds between the metastable crystal structure and the amorphous phase. Therefore data storage does not involve the more stable, hexagonal structures that many phase change alloys possess[8]-[10] which are characterized by a layerwise atomic arrangement of Ge, Sb and Te atoms.

In the metastable rocksalt structure of $\text{Ge}_2\text{Sb}_2\text{Te}_5$ the Te atoms occupy one octahedral lattice site, while Ge and Sb atoms as well as vacancies occupy the second octahedral lattice site[11]. There is hence a concentration of 20% of vacancies on the second (Ge/Sb) lattice site in the (distorted) rocksalt structure. Up to now only very little is known about vacancies in Te alloys. In a very recent publication Edwards et al.[12] demonstrate that vacancies on the Ge sublattice in GeTe are the most easily formed defect and can be created with low formation energies. These vacancies are responsible for the p-type conduction in GeTe. One of the most remarkable features of phase change alloys is threshold switching, a transition of the conductivity in the amorphous state, which proceeds on a sub-nanosecond time scale[13]. This switching mechanism is supposedly related to defects[14], raising the question if there is a relationship between the defects[15] involved in threshold switching and vacancies. The ideas outlined here give ample evidence that a more thorough understanding of the role of vacancies is a necessity for an in-depth understanding of phase change materials.

Matsunaga et al.[16] have investigated the role of vacancies for "GeSbTe" alloys investigating the behaviour of alloys on the GeTe - Sb_2Te_3 tie line. They argue that vacancies in alloys along this tie line should be an intrinsic feature of the structures and relate their appearance with the p-band occupation. In this paper we investigate the role of composition for "GeSbTe" alloys by a computational approach, namely by investigating systems with varying amounts of Ge, Sb and Te vacancies using ab initio density-functional theory.

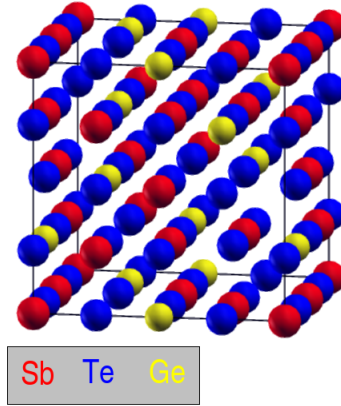


Figure 1: Rocksalt structure of $\text{Ge}_1\text{Sb}_2\text{Te}_4$: Sublattice A consists of Te atoms (blue) while sublattice B consists of 50% Sb atoms (red), 25% Ge atoms (yellow) and 25% vacancies.

2 Calculations & Results

Since $\text{Ge}_1\text{Sb}_2\text{Te}_4$ and $\text{Ge}_2\text{Sb}_2\text{Te}_5$ have considerable vacancy concentrations on the Ge/Sb sublattice (Fig. 1), we have investigated the role of vacancies on this particular sublattice. We have started with a hypothetical $\text{Ge}_2\text{Sb}_2\text{Te}_4$ alloy with a rocksalt structure and a total number of 64 atoms (16 atoms of Ge and Sb each, 32 atoms of Te) in the computational supercell. Recent experiments as well as theoretical calculations have found conclusive evidence that the metastable rocksalt structure is accompanied by considerable distortions around the ideal atomic positions of the rocksalt structure in $\text{Ge}_2\text{Sb}_2\text{Te}_5$ [6],[17] and $\text{Ge}_1\text{Sb}_2\text{Te}_4$ [7]. Indeed, allowing such local distortions also reduces the energy of the $\text{Ge}_2\text{Sb}_2\text{Te}_4$ crystal. Nonetheless, in the following all energies will be compared to the energy of the unrelaxed (local high-symmetry) rocksalt structure of $\text{Ge}_2\text{Sb}_2\text{Te}_4$ unless stated otherwise. In subsequent calculations an increasing number of either Ge or Sb atoms were removed from the $\text{Ge}_2\text{Sb}_2\text{Te}_4$ crystal. The formation energies of the obtained stoichiometries were calculated using the following equation:

$$\Delta E = [E_v + n_v E(\text{Ge/Sb})] - E(\text{Ge}_2\text{Sb}_2\text{Te}_4) \quad (1)$$

Here $E(\text{Ge}_2\text{Sb}_2\text{Te}_4)$ and E_v denote the total energies of the supercells with the original composition $\text{Ge}_2\text{Sb}_2\text{Te}_4$ and of the composition resulting from the removal of Ge or Sb atoms. Furthermore $E(\text{Ge/Sb})$ is the energy of the respective crystalline reservoir of Ge or Sb while n_v denotes the number of vacancies created upon the removal of the atoms. The results are displayed in the upper portion of Fig. 2 for the removal of Ge atoms, where data are both shown for structurally unrelaxed and relaxed rocksalt structures. The energy of the crystal lowers upon removing Ge atoms from the $\text{Ge}_2\text{Sb}_2\text{Te}_4$ crystal, in striking contrast to the behaviour in Si or GaAs where vacancy formation energies are large and positive. Fig. 2 also shows that it is even favourable to remove several Ge atoms from the $\text{Ge}_2\text{Sb}_2\text{Te}_4$ supercell, and 4 Ge vacancies yielding a composition of $\text{Ge}_{1.5}\text{Sb}_2\text{Te}_4$ are most favourable. A second point apparent from Fig. 2 is that lattice distortions also play a crucial role. They lead to a considerable further reduction in energy. Interestingly enough, the energy gain upon the lattice distortions increases with increasing number of Ge vacancies, once more than 4 Ge atoms have been removed. In subsequent calculations we have computed the change in energy upon removal of Sb atoms as well. The resulting data are displayed in the lower part of Fig. 2. Quite similar to the case of Ge removal, the total energy of the $\text{Ge}_2\text{Sb}_2\text{Te}_4$ phase is also lowered by the removal of Sb atoms. In this case 5-6 Sb atoms are missing for the lowest energy within the ideal rocksalt lattice. The energy further lowers upon relaxation. Clearly, the removal of Sb atoms is favoured over the removal of Ge atoms. On the other side, removal of Te atoms increases the energy (data not shown here). Hence our analysis of $\text{Ge}_2\text{Sb}_2\text{Te}_4$ reveals that the total energy of the "GeSbTe" systems is controlled by two different mechanisms: 1) Spontaneous expelling of large amounts of Ge or Sb atoms and 2) local distortions of the rocksalt lattice, both lowering the total energy by similar amounts. Both of them can be understood within one

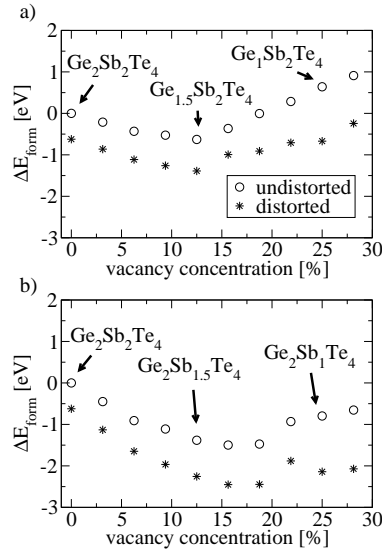


Figure 2: Formation energies for a) Ge and b) Sb vacancies for different concentrations of vacancies: Negative values for the formation energies mean that the respective compound is energetically preferred. The removal of Ge atoms as well as the distortions lower the energy of the crystal on the order of half an eV per supercell.

conceptual framework in terms of the bonding/antibonding states and their associated energies. This can be deduced from quantum chemical computations. Fig. 3 displays the Crystal Orbital Hamilton Population (COHP) curves[18] of the covalent Ge-Te and Sb-Te interactions in the structures of $\text{Ge}_2\text{Sb}_2\text{Te}_4$, $\text{Ge}_{1.5}\text{Sb}_2\text{Te}_4$ and $\text{Ge}_1\text{Sb}_2\text{Te}_4$ both in the ideal (unrelaxed) NaCl-type lattice (top) as well as after the structural relaxation (bottom). The composition $\text{Ge}_2\text{Sb}_2\text{Te}_4$ is characterized by both massively antibonding Ge-Te and Sb-Te interactions in the highest occupied bands close to the Fermi level (horizontal line). Thus, the composition $\text{Ge}_2\text{Sb}_2\text{Te}_4$ stands for a too high valence-electron concentration (VEC) which must be lowered to achieve better stability. The decrease of the VEC by including vacancies furthermore results in a lower charge carrier density. $\text{Ge}_2\text{Sb}_2\text{Te}_4$ exhibits a high density of antibonding states at the Fermi level and thus a high concentration of free carriers. In $\text{Ge}_{1.5}\text{Sb}_2\text{Te}_4$ this density is significantly lower while for $\text{Ge}_1\text{Sb}_2\text{Te}_4$ it decreases even further such that the COHP shows no states at the Fermi level. A simple chemical argument explains why these excess electrons cannot be removed by expelling tellurium atoms. It is the "anionic" Te atom (with a high absolute electronegativity $\chi = 5.49$ eV) whose orbital contributions are dominant in the lower-lying valence band whereas the "cationic" Ge and Sb atoms ($\chi = 4.6$ and 4.85 eV, respectively)[19] mix in mostly in the frontier bands, i.e., where the too high VEC must be lowered. Thus, expelling Te atoms immediately weakens low-lying bonding states and is energetically unfavourable. The comparison with the COHPs of the (unrelaxed) compositions $\text{Ge}_{1.5}\text{Sb}_2\text{Te}_4$ and $\text{Ge}_1\text{Sb}_2\text{Te}_4$ (Fig. 3, top) shows that these antibonding interactions are getting smaller and eventually vanish upon compositional thinning of the cationic substructure.

Upon structural relaxation (Fig. 3, bottom), the band gap between the valence and conduction band increases significantly, thereby mirroring the local structure optimization by "healing" the structural neighbourhood around the empty Ge site, mostly due to the Peierls instability of the Te atom. Where does this optimum composition $\text{Ge}_{1.5}\text{Sb}_2\text{Te}_4$ arise from? A numerical bond-strength COHP analysis yields that, in going from $\text{Ge}_2\text{Sb}_2\text{Te}_4$ to $\text{Ge}_{1.5}\text{Sb}_2\text{Te}_4$ to $\text{Ge}_1\text{Sb}_2\text{Te}_4$, the Ge-Te bonds strengthen by 2 and 8% while the Sb-Te bonds strengthen by 5 and 17% because antibonding states are emptied. The optimum composition (= $\text{Ge}_{1.5}\text{Sb}_2\text{Te}_4$), however, is also determined by the absolute number of Ge-Te bonds (25% fewer for $\text{Ge}_{1.5}\text{Sb}_2\text{Te}_4$, 50% fewer for $\text{Ge}_1\text{Sb}_2\text{Te}_2$) and Sb-Te bonds (constant) upon expelling Ge atoms from the crystal. Thus, the energetic gain by emptying antibonding states favors the Ge-poor composition $\text{Ge}_1\text{Sb}_2\text{Te}_2$ which refers to the abovementioned point (a), while maintaining a maximum number of Ge-Te bonds -referring to point (b) - strives for the Ge-rich $\text{Ge}_2\text{Sb}_2\text{Te}_4$; the energetic compromise arrives at $\text{Ge}_{1.5}\text{Sb}_2\text{Te}_4$. For expelling Sb atoms, analogous arguments apply. In the following we will discuss the mechanism driving the further structural distortion in more detail. To understand its nature Fig. 4 displays the pair correlation functions for Ge, Sb and Te for three different alloys ($\text{Ge}_2\text{Sb}_2\text{Te}_4$, $\text{Ge}_{1.5}\text{Sb}_2\text{Te}_4$ and $\text{Ge}_1\text{Sb}_2\text{Te}_4$) in the distorted rocksalt structure. Two findings are apparent from this figure: 1) There are pronounced local distortions for the nearest neighbour Ge-Te bonds, which lead to a splitting

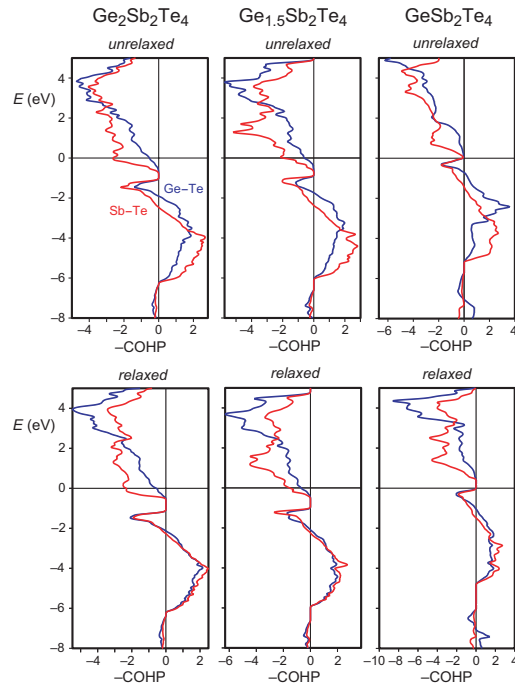


Figure 3: Crystal-Orbital Hamilton Population (COHP) bonding analysis: The plot displays the Ge-Te (blue) and Sb-Te (red) interactions in $\text{Ge}_2\text{Sb}_2\text{Te}_4$ (left), $\text{Ge}_{1.5}\text{Sb}_2\text{Te}_4$ (middle) and GeSb_2Te_4 (right); the upper panel shows the situation in the undistorted NaCl-like lattice whereas the lower panel corresponds to the structure with full atomic relaxation. The Fermi levels were set to the energy zero. Bonding interactions to the right, antibonding interactions to the left.

of those bonds in shorter and longer Ge-Te bonds. A similar finding is observed for the Sb-Te bonds, even though the splitting into shorter and longer bonds is less pronounced. Such a splitting into shorter and longer bonds is often denoted as a Peierls effect[20]. 2) Comparing the three different alloys it is apparent that the size of the local distortions changes with composition. The distortions are smallest for $\text{Ge}_2\text{Sb}_2\text{Te}_4$ with an average value of 0.1 Å, intermediate for $\text{Ge}_{1.5}\text{Sb}_2\text{Te}_4$ (0.13 Å) and are largest for GeSb_2Te_4 (0.18 Å). The values for the distortions denote the average deviation of the bond length in the distorted structure from the bond length in the undistorted rocksalt structure. In Fig. 4 the decrease and broadening of the next-neighbour peaks demonstrates the increase of the distortions with increasing number of vacancies. Such a finding is indicative for an interplay between vacancies on the one side and distortions on the other in "GeSbTe" crystals.

The bonding of these chalcogenide alloys is mainly governed by their p -orbitals. The three orthogonal p atomic orbitals overlap and allow the construction of the ideal rocksalt structure. According to Peierls[21], however, the perfect rocksalt structure is unstable against local distortions, accompanied by an opening or widening of the electronic band gap, given a proper band filling. A similar finding also results for the three computational models $\text{Ge}_2\text{Sb}_2\text{Te}_4$, $\text{Ge}_{1.5}\text{Sb}_2\text{Te}_4$ and GeSb_2Te_4 . The low coordination number in the relaxed/distorted systems results in non-bonding electronic states. Elemental Te, for instance, has four valence p electrons but is only twofold coordinated, a consequence of the Peierls instability of the simple cubic structure[22]. Thus, one p -orbital can be described as a nonbonding orbital filled with two electrons[23]. Germanium on the other hand, exhibits one completely empty p -orbital. In the simplest possible interpretation, adding germanium to an Sb-Te alloy therefore reduces the number of these non-bonding states because the bonding between the Te lone pair and this empty Ge orbital results in an energetically favourable configuration compared to a system that exhibits non-bonding states. Thus adding Ge to GeSb_2Te_4 , on one side, reduces the energy gain by the Peierls distortion but it is energetically favourable, on the other side, as it reduces the number of non-bonding Te states. However, the addition of a large amount of Ge atoms to GeSb_2Te_4 becomes unfavourable as anti-bonding states above the Fermi energy are occupied in that case. Along the $\text{Ge}_2\text{Sb}_2\text{Te}_4$ - $\text{Ge}_2\text{Sb}_1\text{Te}_4$ series analogous arguments apply. Since Sb has more p electrons than Ge, however, it is less effective in reducing the number of Te lone pairs which thereby leads to a more pronounced occupation of antibonding states. Therefore, the optimal configuration is found for a higher number of vacancies than along the $\text{Ge}_2\text{Sb}_2\text{Te}_4$ - GeSb_2Te_4 series.

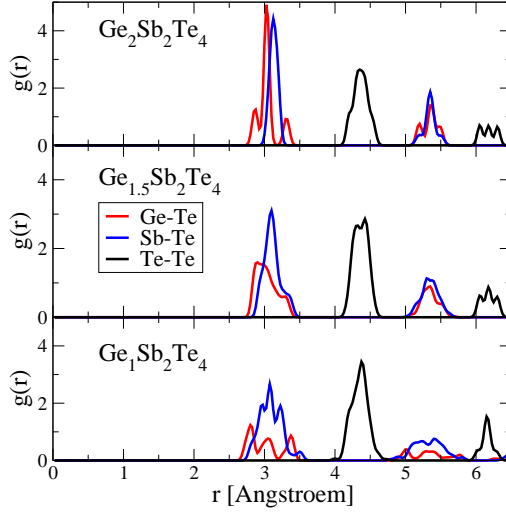


Figure 4: Pair correlation functions for $\text{Ge}_2\text{Sb}_2\text{Te}_4$ (top), $\text{Ge}_{1.5}\text{Sb}_2\text{Te}_4$ (middle) and $\text{Ge}_1\text{Sb}_2\text{Te}_4$ (bottom). All systems have been structurally relaxed. A broadening of the Ge-Te and Sb-Te peaks is observed. The size of the effect increases with vacancy concentrations.

Until now it has always been argued in the literature that the most stable "GeSbTe" based phase change materials are those that are situated on the GeTe-Sb₂Te₃ pseudobinary line such as GeTe, Ge₁Sb₂Te₄ and Ge₂Sb₂Te₅. However, Fig. 2 shows that in the metastable rocksalt-like phase Ge_{1.5}Sb₂Te₄ and Ge₂Sb_{1.33}Te₄ form the most stable crystalline states when either Ge or Sb vacancies, respectively are considered. Both phases are more stable than Ge₁Sb₂Te₄. This first of all indicates that both alloys have a higher resistance against phase separation which should lead to a better stability upon multiple rewriting cycles.

In order to prove the predicted stability of the calculated compositions and to analyze their physical properties we have employed Ge_{1.5}Sb₂Te₄, Ge₂Sb₂Te₄ and Ge₂Sb₁Te₄ sputter targets. Using these compounds, thin films were sputtered and compared with films of the commonly studied phase change alloys Ge₁Sb₂Te₄ and Ge₂Sb₂Te₅. Both of these alloys are found on the pseudo-binary GeTe-Sb₂Te₃ line. The as deposited films are amorphous, the crystallization temperature increases along the Ge₁Sb₂Te₄-Ge₂Sb₂Te₄ line (see Table 1), indicating a higher overall stability with increasing Ge content. The crystallization temperature of Ge₂Sb₁Te₄ is similar to Ge₂Sb₂Te₅ but higher than Ge₁Sb₂Te₄.

The metastable crystalline phase of all the novel alloys shows the characteristic peaks of the rocksalt structure with lattice parameters of around 6 Å (Fig. 5 and Table 1) and no evidence for phase separation. A striking result is found for the optical contrast between the amorphous and metastable crystalline state. Fig. 6(a) shows the absorption spectra for Ge₁Sb₂Te₄, Ge_{1.5}Sb₂Te₄, Ge₂Sb₂Te₄ and Ge₂Sb₁Te₄. While the curves are very similar in the amorphous phase, the absorption intensity increases significantly in the crystalline phase if we move from Ge₁Sb₂Te₄ to Ge_{1.5}Sb₂Te₄ and further to Ge₂Sb₂Te₄. The optical contrast for Ge_{1.5}Sb₂Te₄ and Ge₂Sb₁Te₄ is similar. The optical contrast - which is of great importance for the optical data storage application of phase change materials - in the novel compositions Ge_{1.5}Sb₂Te₄, Ge₂Sb₁Te₄ and in particular Ge₂Sb₂Te₄ is therefore significantly more pronounced than in Ge₁Sb₂Te₄. This proves that the amount of vacancies and the degree of the structural distortions are of greater importance for the optical properties in the crystalline phase than in the amorphous phase. As it is comparatively easy to study the crystalline phase - both

	Ge ₁ Sb ₂ Te ₄	Ge _{1.5} Sb ₂ Te ₄	Ge ₂ Sb ₂ Te ₄	Ge ₂ Sb ₁ Te ₄	Ge ₂ Sb ₂ Te ₅
T _c [C]	145	169	175	158	157
E _a [eV]	2.64 ± 0.05	2.54 ± 0.15	2.73 ± 0.13	2.42 ± 0.15	2.23 ± 0.07
a [Å]	6.043	6.000 ± 0.001	6.003 ± 0.002	5.969 ± 0.002	6.000 ± 0.002

Table 1: Crystallization temperature, activation energy against crystallization and the crystal structure of the metastable phase for the GST alloys. All these measurements have been performed with alloys in the as deposited state.

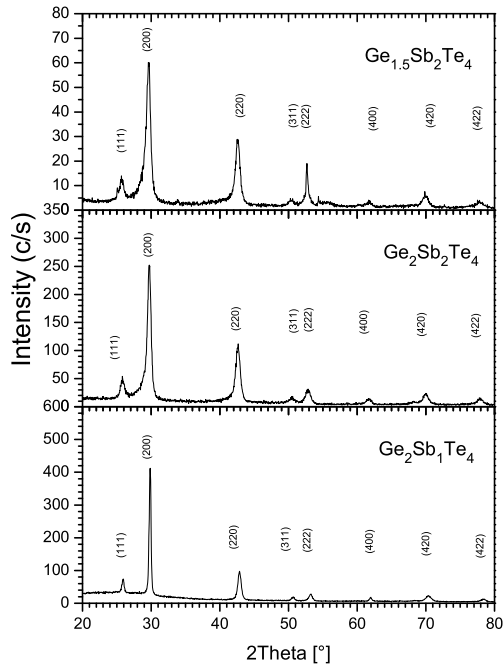


Figure 5: XRD diffractograms of $\text{Ge}_{1.5}\text{Sb}_2\text{Te}_4$, $\text{Ge}_2\text{Sb}_2\text{Te}_4$ and $\text{Ge}_2\text{Sb}_1\text{Te}_4$: The diffractograms show a metastable phase after crystallization from the as deposited amorphous phase. The peaks have been identified and attributed to the metastable rocksalt structure.

with experimental as well as with computational methods - and correlate structural with electronic and optical properties, this finding represents an important result for further studies of novel phase change alloys for applications in optical data storage. The suitability of any phase change alloy is determined also by the rapid and reversible phase transformation. The time limiting step in optical recording is recrystallization[24], which was investigated for all new alloys. In Fig. 6(b) we present the recrystallization results of the $\text{Ge}_{1.5}\text{Sb}_2\text{Te}_4$ alloy. The color codes indicate the reflectivity level after the passage of the second pulse. It is clearly seen that complete recrystallization proceeds after 30 ns and this is comparable to the values of the widely used $\text{Ge}_2\text{Sb}_2\text{Te}_5$ alloy (10 ns)[25],[26].

3 Conclusions

To our knowledge this is the first time that a phase change alloy with superior properties for optical data storage has been first developed by advanced calculations and subsequently been produced and tested experimentally. This accomplishment has been enabled by a detailed understanding of the nature of bonding in GST based alloys, in particular the delicate interplay between p electron band filling, antibonding states and optimum Peierls distortions. Once a microscopic model for electric switching has been established, the model outlined above could possibly also be applied to develop new materials for electronic data storage.

References

- [1] El-Mellouhi, F., Mousseau, N. & Ordejon, P. Sampling the diffusion paths of a neutral vacancy in silicon with quantum mechanical calculations. *Phys. Rev. B* **70**, 205202 (2004).
- [2] Yamada, N. Erasable phase-change optical materials. *MRS Bull.* **21**, 48–50 (1996).
- [3] Ovshinsky, S. R. Reversible electrical switching phenomena in disordered structures. *Phys. Rev. Lett.* **21**, 1450–1453 (1968).

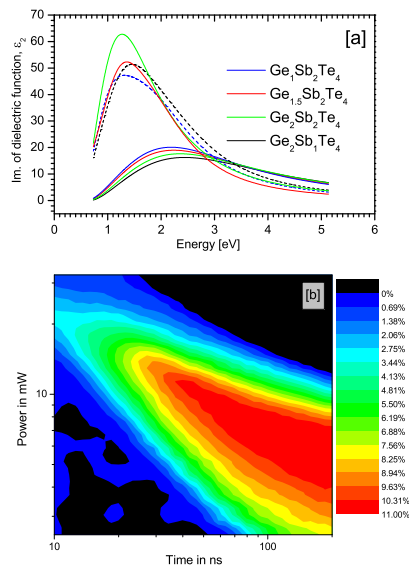


Figure 6: Optical properties and recrystallization behaviour: In (a) the imaginary part of the dielectric function is presented for the amorphous (solid lines) and crystalline phases (broken lines) of the $\text{Ge}_1\text{Sb}_2\text{Te}_4$ - $\text{Ge}_2\text{Sb}_2\text{Te}_4$ alloys and of $\text{Ge}_2\text{Sb}_1\text{Te}_4$. There is a systematic increase in absorption with decreasing Ge and Sb vacancy concentrations. (b): Power Time Effect diagram to show the recrystallization of the $\text{Ge}_{1.5}\text{Sb}_2\text{Te}_4$ alloy after laser amorphisation: We used a pre-pulse of fixed power and duration to amorphize and a variable post-pulse to crystallize the written bit. The effect of the laser is seen as a change in reflectivity after applying the second pulse. The colour codes show the reflectivity change of the laser induced amorphous bit. The crystallization event leads to an increase in reflectivity and thus it is observed that complete recrystallization commences after 30 ns.

- [4] Wuttig, M. Phase-change materials - towards a universal memory? *Nature Materials* **4**, 265–266 (2005).
- [5] Lankhorst, M., Ketelaars, B. & Wolters, R. Low-cost and nanoscale non-volatile memory concept for future silicon chips. *Nature Materials* **4**, 347–352 (2005).
- [6] Kolobov, A. *et al.* Understanding the phase-change mechanism of rewritable optical media. *Nature Materials* **3**, 703–708 (2004).
- [7] Welnic, W. *et al.* Unraveling the interplay of local structure and physical properties in phase-change materials. *Nature Materials* **5**, 56–62 (2006).
- [8] Matsunaga, T. & Yamada, N. Structural investigation of $\text{Ge}_1\text{Sb}_2\text{Te}_4$: A high-speed phase-change material. *Phys. Rev. B* **69**, 104111 (2004).
- [9] Kooi, B., Groot, W. & de Hosson, J. In situ transmission electron microscopy study of the crystallization of $\text{Ge}_2\text{Sb}_2\text{Te}_5$. *J. Appl. Phys.* **95**, 924–932 (2004).
- [10] Abrikosov, N. & Danilova-Dobryakova, G. Study of the Sb,Te,-GeTe phase diagram. *Izv.Akad. Nauk.SSSR, Neorg. Mater.* **1**, 204–209 (1965).
- [11] Matsunaga, T., Kubota, Y. & Yamada, N. Structures of stable and metastable $\text{Ge}_2\text{Sb}_2\text{Te}_5$, an intermetallic compound in the GeTe-Sb₂Te₃ pseudobinary systems. *Acta Cryst. B* **60**, 685–691 (2004).
- [12] Edwards, A. H. *et al.* Electronic structure of intrinsic defects in crystalline germanium telluride. *Phys. Rev. B* **73**, 045210 (2006).

- [13] Adler, D., Shur, M. & Ovshinsky, S. Threshold switching in chalcogenide-glass thin films. *J. Appl. Phys.* **51**, 3289–3309 (1980).
- [14] Pirovano, A., Lacaita, A., Benvenuti, A., Pellizzer, F. & Bez, R. Electronic switching in phase-change memories. *Electron Devices, IEEE Transactions on* **51**, 452 – 459 (2004).
- [15] Baranovskii, S. & Karpov, V. Localized electron states in glassy semiconductors (review). *Sov. Phys. Semicond.* **21**, 1–10 (1987).
- [16] Matsunaga, T. *et al.* Single structure widely distributed in a GeTe-Sb₂Te₃ pseudobinary system: A rocksalt structure is retained by intrinsically containing an enormous number of vacancies within its crystal. *Inorg. Chem* **45**, 2235–2241 (2006).
- [17] Shamoto, S. *et al.* Large displacement of germanium atoms in crystalline Ge₂Sb₂Te₅. *Appl. Phys. Lett.* **86**, 081904 (2005).
- [18] Dronskowski, R. & Blöchl, P. Crystal orbital hamilton populations (cohp): energy-resolved visualization of chemical bonding in solids based on density-functional calculations. *J. Phys. Chem.* **97**, 8617 – 8624 (1993).
- [19] Pearson, R. Absolute electronegativity and hardness: application to inorganic chemistry. *Inorg. Chem.* **27**, 734 – 740 (1988).
- [20] Gaspard, J.-P. & Ceolin, R. Hume-rothery rule in V- VI compounds. *Sol. State Comm.* **84**, 839–842 (1992).
- [21] Peierls, R. *Quantum theory of solids* (Oxford University Press, 1956).
- [22] Decker, A., Landrum, G. & Dronskowski, R. Structural and electronic peierls distortions in the elements (A): The crystal structure of tellurium. *Z. Anorg. Allg. Chem.* **628**, 295–302 (2002).
- [23] Kastner, M. Bonding bands, lone-pair bands, and impurity states in chalcogenide semiconductors. *Phys. Rev. Lett.* **28**, 355–357 (1972).
- [24] Zhou, G. Material aspects in phase change optical recording. *Mat. Sci. and Eng. A* **304-306**, 73–80 (2001).
- [25] Borg, H., Lankhorst, M., Meinders, E. & Leibbrandt, W. Phase change media for high density optical recording. *Mat. Res. Soc. Symp. Proc* **674**, V1.2.1–10 (2001).
- [26] Wuttig, M. *et al.* The quest for fast phase change materials. *Mat. Res. Soc. Symp. Proc* **674**, V1.8–16 (2001).

Biography Wojciech Welnic

- since 07/2007: Feodor-Lynen-Fellow of the Alexander von Humboldt-Foundation at the Laboratoire des Solides Irradiés, École Polytechnique in Palaiseau, France and at the ESRF, Grenoble, France. Research topic: Electronic and structural properties of phase change materials with Time-Dependent Density Functional Theory and Inelastic X-Ray Scattering
- 08/2006 – 03/2007: Post-doctoral fellow at the I. Physikalisches Institut (Institute for New Materials), RWTH Aachen University, Germany
- 04/2003 – 08/2006: PhD thesis in Physics at the I. Physikalisches Institut (Institute for New Materials), RWTH Aachen University, Germany, Title: “Electronic and Optical Properties of Phase Change Alloys revealed with *ab initio* Methods”, Supervisor: Prof. Dr. Matthias Wuttig
- 11/2003 – 09/2004: Research stay at the Laboratoire des Solides Irradiés, École Polytechnique in Palaiseau, France, Supervisor: Dr. Lucia Reining
- 04/2003 – 10/2003: Research stay at the Institut für Festkörperforschung, Forschungszentrum Jülich, Germany, Supervisor: Prof. Dr. Stefan Blügel